Mass Spectrometry Analysis of Recombinant Human ZP3 Expressed in Glycosylation-Deficient CHO Cells

Ming Zhao,[‡,§] Emily S. Boja,[‡,||] Tanya Hoodbhoy,[§] Joseph Nawrocki,[⊥] Jeanne B. Kaufman,[§] Nicole Kresge,[§] Rodolfo Ghirlando,[#] Joseph Shiloach,[§] Lewis Pannell,[⊥] Rodney L. Levine,[△] Henry M. Fales,[||] and Jurrien Dean*[,§]

Laboratory of Cellular and Developmental Biology, Laboratory of Bioorganic Chemistry, and Laboratory of Molecular Biology, NIDDK, and Laboratory of Biophysical Chemistry and Laboratory of Biochemistry, NHLBI, National Institutes of Health, Bethesda, Maryland 20892

Received May 21, 2004; Revised Manuscript Received July 23, 2004

ABSTRACT: The zona pellucida is an extracellular matrix that mediates taxon-specific fertilization in which human sperm will not bind to mouse eggs. The mouse zona pellucida is composed of three glycoproteins (ZP1, ZP2, ZP3). The primary structure of each has been deduced from the cDNA nucleic acid sequence, and each has been analyzed by mass spectrometry. However, determination of the secondary structure and processing of the human zona proteins have been hampered by the paucity of biological material. To investigate if taxon-specific sperm−egg recognition was ascribable to structural differences in a zona protein required for matrix formation, recombinant human ZP3 was expressed in CHO-Lec3.2.8.1 cells and compared to mouse ZP3. With nearly complete coverage, LC−QTOF mass spectrometry was used to determine the cleavage of an N-terminal signal peptide (amino acids 1−22) and the release of secreted ZP3 from a C-terminal transmembrane domain (amino acids 379−424). The resultant N-terminal glutamine was cyclized to pyroglutamate (pyrGln^{23}), and several C-terminal peptides were detected, including one ending at Asn^{350}. The disulfide bond linkages of eight cysteine residues in the conserved zona domain were ascertained (Cys^{46}/Cys^{140}, Cys^{78}/Cys^{99}, Cys^{217}/Cys^{282}, Cys^{239}/Cys^{300}), but the precise linkage of two additional disulfide bonds was indeterminate due to clustering of the remaining four cysteine residues (Cys^{319}, Cys^{321}, Cys^{322}, Cys^{327}). Three of the four potential N-linked oligosaccharide binding sites (Asn^{125}, Asn^{147}, Asn^{272}) were occupied, and clusters of O-glycans were observed within two regions, amino acids 156−173 and 260−281. Taken together, these data indicate that human and mouse ZP3 proteins are quite similar, and alternative explanations of taxon-specific sperm binding warrant exploration.

The zona pellucida (ZP)[1] is an extracellular matrix that surrounds growing oocytes, ovulated eggs, and preimplantation embryos. The zona provides a structural framework for interactions between somatic and germ cells during folliculogenesis, mediates taxon-specific sperm binding to the egg, provides a potent postfertilization block to polyspermy, and is critical for the successful transit of the developing embryo through the oviduct (*1*). Similar egg envelopes have been described in all vertebrates, and individual envelope proteins are well conserved. Mouse zonae pellucidae contain three major glycoproteins (ZP1, ZP2, ZP3), and human homologues to ZP2 and ZP3 have been characterized (*2*, *3*). A third human protein, ZPB, more distantly related to mouse ZP1, has been identified (*4*), and analysis of the human genome indicates a fourth human protein (homologue of mouse ZP1) as well (*5*).

The primary structure of the mouse and human zona proteins has been deduced from the nucleic acid sequence of full-length cDNA clones (for review see ref *6*). Each has a computer-predicted signal peptide that directs it into a secretory pathway, and each has a putative transmembrane domain near its carboxyl terminus. The latter suggests that each protein is tethered to a membrane prior to its release and incorporation into the insoluble extracellular zona pellucida matrix. All zona proteins also have a 260 amino acid zona domain with 8 conserved cysteine residues (*7*) that is located toward the carboxyl terminus of ZP1 and ZP2 and occupies much of the smaller ZP3 protein. Similar motifs have been noted in α- and β-tectorins that form an extracellular matrix in the inner ear (*8*, *9*), suggesting a central role for the zona domain in protein−protein interactions of extracellular matrices (*10*). Recent genetic studies demon-

* To whom correspondence should be addressed. Tel: (301) 496-2738. Fax: (301) 496-5239. E-mail: jurrien@helix.nih.gov.
‡ These authors contributed equally to the work.
§ Laboratory of Cellular and Developmental Biology, NIDDK.
|| Laboratory of Biophysical Chemistry, NHLBI.
⊥ Laboratory of Bioorganic Chemistry, NIDDK.
Laboratory of Molecular Biology, NIDDK.
△ Laboratory of Biochemistry, NHLBI.

[1] Abbreviations: ZP, zona pellucida; AEBSF, (aminoethyl)benzenesulfonyl fluoride; CHO, Chinese hamster ovary; CID, collision-induced dissociation; DMEM, Dulbecco/Vogt-modified Eagle's medium; DTT, dithiothreitol; EDTA, ethylenediaminetetraacetic acid; FPLC, fast-performance liquid chromatography; FBS, fetal bovine serum; GalNAc, *N*-acetylgalactosamine; GlcNAc, *N*-acetylglucosamine; HEPES, 4-(2-hydroxyethyl)piperazine-1-ethanesulfonic acid; Hex, hexose; HexNAc, *N*-acetylhexose; ITMS, ion trap mass spectrometry; LC−QTOF, liquid chromatography−quadrupole time of flight; MALDI, matrix-assisted laser desorption/ionization; MEM, minimum essential medium; MS, mass spectrometry; NANA, *N*-acetylneuraminic acid; PBS, phosphate-buffered saline; PNGase F, peptide *N*-glycosidase F; SDS−PAGE, sodium dodecyl sulfate−polyacrylamide gel electrophoresis.

10.1021/bi048958k
Published on Web 09/01/2004

strate that mice lacking ZP1 form a structurally defective zona pellucida composed of ZP2 and ZP3 (*11*) and mice lacking ZP2 initially form a thin matrix early in folliculogenesis that does not persist in ovulated eggs (*12*). Thus, it appears that either ZP1/ZP3 or ZP2/ZP3 dimers can form a zona matrix, although the latter is considerably more enduring than the former. However, mice lacking ZP3 never acquire a visible zona matrix (*13*, *14*), indicating its essential role in forming the extracellular zona pellucida matrix.

Particular interest has focused on the role of the zona pellucida in fertilization. Sperm bind and penetrate the zona pellucida of eggs, but not two-cell embryos, and credible models of sperm−egg recognition must account for this dichotomy. Over the last two decades, the molecular basis of sperm binding to the zona pellucida has been variously ascribed to single zona proteins, single terminal N- or O-glycans that are removed following fertilization, and supramolecular structures that are rendered nonpermissive for sperm binding by the postfertilization cleavage of ZP2 (for reviews see refs *15*−*17*). Although there is no compelling reason for species-specific gamete interactions among internally fertilizing mammals, there is some taxon specificity to sperm−egg recognition. If the three-dimensional structures of mouse and human zona proteins were sufficiently different, they might account for the inability of human sperm to bind to mouse eggs acting either as an individual protein or as modulators of supramolecular structures within the zona matrix.

The proteins of the native mouse zona pellucida have been previously analyzed by mass spectrometry (*18*), but the difficulty in obtaining biological material precludes a similar analysis of native human zona proteins. As noted, ZP3 is required for the formation of the zona pellucida matrix. Therefore, taking advantage of earlier success in expressing mouse ZP3 in CHO cells (*19*), human ZP3 has been expressed in glycosylation-deficient CHO cells (*20*) to minimize heterogeneity and analyzed by microscale mass spectrometry.

EXPERIMENTAL PROCEDURES

Stable Cell Lines Expressing Human ZP3. Full-length human ZP3 cDNA (*3*) was cloned into the *Eco*RI site of the expression vector pEF1/V5-His (version A; Invitrogen, Carlsbad, CA) downstream of the EF-1α promoter. The insertion and correct orientation were confirmed by restriction enzyme digestion with *Aat*II and *Sca*I. Glycosylation-deficient CHO cells (CHO-Lec3.2.8.1; gift of Dr. Pamela Stanley) were cultured with αMEM (minimum essential medium, alpha) (Invitrogen, Carlsbad, CA) supplemented with 10% FBS (*20*). Transfection of the cells with the expression vector was performed using Lipofectamine plus reagent (Invitrogen, Carlsbad, CA) according to the manufacturer's instructions. After 2 days of culture, Geneticin (400 μg/mL) was added to the media, the cells were split (1:500), and positive clones were isolated 1 week later.

Expression of Recombinant Human ZP3. Recombinant human ZP3 was produced in a continuous culturing system by immobilizing the stably transformed CHO-Lec3.2.8.1 cells in a packed-bed configuration using a 2.2 L (1.6 L working volume) bioreactor equipped with a vertical mixing impeller assembly and an internal basket (*21*). Initially, stably transfected CHO-Lec3.2.8.1 cells (*20*) were cultured with αMEM supplemented with 10% FBS and Geneticin (200 μg/mL). The cells were split and transferred into defined CHO-SFM II medium (Invitrogen, Carlsbad, CA), 2.5% FBS, and Geneticin (200 μg/mL) via two intermediate changes: 50% MEM + 50% SFM II with 5% FBS, and 25% MEM + 75% SFM II with 2.5% FBS, both supplemented with Geneticin (200 μg/mL). Approximately 8×10^8 cells were then seeded into the internal basket of the bioreactor that contained 60 g of Fibra-cel disks (Bibby Sterlin, U.K.) made of polyester nonwoven fabric laminated to a polypropylene screen treated and precoated with poly(D-lysine). The culture was maintained at 37 °C, pH 7.0, and dissolved oxygen concentration was maintained at 50% air saturation by sparging with air. Cell growth was monitored by glucose consumption, and the pH was maintained by the addition of 1 M sodium hydroxide.

Preparation of the H3.1 Antibody Affinity Column. H3.1 antibody specific to human ZP3 (*22*) was purified from a hybridoma cell line cultured with DMEM, 20% low IgG FBS (Hyclone Laboratories, Logan, UT), and HIPO (50 μg/mL sodium pyruvate, 150 μg/mL oxaloacetic acid, 0.2 unit/mL insulin, 2.38 mg/mL HEPES, 3.5 nL/mL β-mercaptoethanol, adjusted to pH 7.0 with potassium hydroxide). After 1 week of culture, the supernatant was centrifuged to remove cellular debris and applied to a goat anti-mouse IgG (H + L)−Sepharose 4B (Zymed Laboratories, South San Francisco, CA) affinity column. The column was washed with PBS (10 bed volumes), and the bound mouse antibody was eluted with 0.1 M citric acid−0.2 M sodium phosphate, pH 3.5. The pH of the eluted fractions was quickly neutralized by adding sodium bicarbonate. Fractions containing H3.1 were dialyzed against 0.2 M sodium bicarbonate, pH 8.3, containing 0.5 M sodium chloride and concentrated with a Centriprep-30 (Millipore, Bedford, MA). Approximately 30 mg of antibody was obtained from 1 L of cell culture supernatant. The purity of the antibody was assayed by SDS−PAGE stained with Coomassie Brilliant Blue G, and its identity was confirmed by immunoblot analysis. The purified H3.1 monoclonal antibodies were then coupled to a 5 mL Hi-trap NHS-activated Sepharose column (Amersham-Pharmacia Biotech, Piscataway, NJ) according to the manufacturer's instructions.

Purification of Recombinant Human ZP3. Recombinant human ZP3 was purified sequentially by antibody affinity, ion-exchange, and gel filtration chromatography performed at 4 °C (Supporting Information, Figure 1C, panel 1).

H3.1 Antibody Affinity Chromatography. Twenty liters of culture media containing recombinant human ZP3 was concentrated by a Millipore cassette system (10000 MWCO; Millipore Corp., Bedford, MA) to 1 L, and protease inhibitors, 1 mM AEBSF, 10 mM EDTA, aprotinin (5 Fg/mL), leupepstin (1 Fg/mL), and pepstatin (1 Fg/mL), were added. Cellular debris was removed by low-speed centrifugation (1000*g*, 10 min), and the remaining media were recentrifuged (13000*g*, 30 min). The supernatant was applied to the Hi-trap-H3.1 affinity column at a flow rate of 1 mL/min, controlled by a peristalic pump (P-100; Pharmacia Biotech). After being washed with 50 mL of PBS, pH 7.4 (10 bed volumes), protein was eluted with 0.1 M citric acid−0.2 M sodium phosphate, pH 3.5. The eluted fractions were

immediately brought to neutral pH by adding 1 M Tris-HCl, pH 8.5.

Hi-Trap Q Ion-Exchange Chromatography. The fractions eluted from the antibody affinity column [4−5 mg of recombinant protein, A_{280} (1 mg/mL) = 1 OD] were dialyzed against 20 mM Tris-HCl, pH 6.8, and applied onto a Hi-trap Q (5 mL) ion-exchange column preequilibrated with the same buffer. Protein was eluted by a sodium chloride concentration gradient (0−1 M) generated by a LCC-501 Plus FPLC system (Pharmacia Biotech). Elution was monitored at A_{280}, and three peaks were observed (Supporting Information, Figure 1C, panel 2). The first peak contained proteins that had bound nonspecifically to the affinity column, and the second contained recombinant human ZP3 (retention time 28−38 min). The third peak did not contain any protein bands as detected by SDS−PAGE and staining with Coomassie Brilliant Blue G.

Superose 12 Gel Filtration Chromatography. Fractions containing human ZP3 from the previous purification step were concentrated by Centricon 10 (Millipore Corp., Bedford, MA) and applied to a Superose 12 (HR 10/30; Pharmacia Biotech) gel filtration column on the FPLC system. Using a flow rate of 0.2 mL/min, recombinant protein eluting between 34.5 and 43.5 min (Supporting Information, Figure 1C, panel 3) was pooled, concentrated with Centricon 10, and applied to the same Superose 12 column for a second fractionation (Supporting Information, Figure 1C, panel 4). The eluted ZP3 fractions (retention time 34.5−43.5 min) were then pooled and concentrated as the final product of purified recombinant human ZP3.

Glycosidase and Protease Treatment. For each glycosidase digestion, recombinant protein (10 μg) was denatured (100 °C, 10 min, 0.5% SDS) and incubated in 50 mM sodium citrate, pH 5.5, at 37 °C for 2 h. For endo-H glycosidase digestion alone, 1 μL of endo-H glycosidase (1000 units; New England Biolabs, Beverly, MA) was added to the denatured proteins. For the combination of endo-H and endo-O glycosidase digestion, 1 μL of endo-H glycosidase, 0.3 μL of endo-O glycosidase (1.25 units/mL; Prozyme, San Leandro, CA), 0.3 μL of sialidase A (5 units/mL; Prozyme), and 1% NP-40 (final) were added to the reaction. For proprotein convertase digestion, ∼200 ng of furin (Alexis Biochemicals, San Diego, CA) was added to denatured protein for 2 h, 37 °C, in 50 mM Tris-HCl, pH 7.5, 1 mM calcium chloride, and 0.1% Triton X-100.

Mass Spectrometry Analysis. A mixture (20−50 μg) of mouse ZP1, ZP2, and ZP3 or recombinant human ZP3 alone was denatured (8 M urea), reduced (5 mM DTT), alkylated (0.5 M iodoacetamide), and de-N and de-exo-O glycosylated using PNGase F and a mixture of exo-O glycosidases [sialidase A, β-(1−4) galactosidase and glucosaminidase], successively, and the samples were treated with trypsin and/or Asp-N endoproteinase (*18*). Duplicate samples were processed without reduction by DTT to determine the pattern of intramolecular disulfide linkages. Sites of N-glycosylation were found by the mass addition of 0.98 Da due to the conversion of asparagine to aspartic acid by PNGase F digestion and confirmed by MS/MS fragmentation. O-Glycosylated serines/threonines were located by treating 10−30 pmol of a de-N and de-exo-O glycosylated sample with trypsin and/or Asp-N endoproteinase, and the sample was either (1) subjected to a lower collisional energy to keep core disaccharide O-glycans attached to Ser/Thr, their site of attachment being identified by IT-CID, or (2) lyophilized and treated with methylamine (100 μL of 40% solution, 4 h, 50 °C) to catalyze β-elimination of core O-glycans and form a stable derivative of the previously O-glycosylated Ser/Thr residues (*23*). The alkylamine was considered to be a label of O-glycosylation sites, and the resultant peptides were subjected to Micromass (Manchester, U.K.) QTOF−CID. Samples (2 pmol) were analyzed by micro-LC mass spectrometry as previously described (*18*).

ESI−LC−Ion Trap Mass Spectrometry (ITMS). Proteolytic peptides were analyzed on a ThermoFinnigan 2D-LC proteome X system in high-throughput 1D mode (ThermoFinnigan, San Jose, CA). The gradient for MS pump (200 μL/min split 1:100 to a final flow rate of 2 μL/min into the mass spectrometer) was as follows: 0−45% solvent B in 40 min, followed by ramping up to 95% solvent B in 5 min; 95% solvent B was held for an additional 5 min (solvent A, 0.1% formic acid in 100% water; solvent B, 0.1% formic acid in 100% acetonitrile). Meanwhile, the sample pump was maintained at 100% solvent C (0.1% formic acid in 95% water/5% acetonitrile) at 200 μL/min (1:100 split to 2 μL/min) throughout the entire run. MS tune parameters were as follows: spray voltage, 3.5 kV; capillary temperature, 180 °C; tube lens, 15 V; capillary voltage, 32 V. For O-glycopeptides, CID using a parent ion inclusion list was performed at 25% collision energy to minimize sugar losses from the peptide backbone.

Sedimentation Equilibrium Ultracentrifugation. Sedimentation equilibrium experiments were performed using a Beckman XL-A analytical ultracentrifuge. Data were acquired as an average of eight absorbance measurements at 280 nm and a radial spacing of 0.001 cm. Experiments were performed at 4 °C and rotor speeds of 10, 12, and 14 krpm in 100 mM sodium chloride, 20 mM Tris-HCl, pH 7.4, and 0.01% sodium azide at loading concentrations corresponding to measured A_{280} of 0.14 and 0.39. Data were analyzed globally in terms of both a single ideal solute and two noninteracting single ideal solutes to obtain the buoyant molecular mass, $M(1 - \upsilon\rho)$, using Sigma Plot 8.0. Experimental masses of the human ZP3 glycoprotein were determined on the basis of the additivities of the protein and carbohydrate partial specific volumes (*24*) in which the partial specific volumes of the protein and carbohydrate components are calculated on the basis of the amino acid composition (*25*) and assumed carbohydrate composition (*26*), respectively.

RESULTS

Purification of Recombinant Human ZP3. Native human ZP3 undergoes extensive posttranslational modifications (*27*), and analysis of its primary structure indicates four potential N-glycosylation (Asn-Xaa-Ser/Thr) sites and 66 potential O-glycosylation sites (Ser or Thr) (*3*). To reduce the degree of heterogeneity of the recombinant protein, human ZP3 cDNA was cloned into the pEF1/V5-His6 expression vector and expressed in CHO-Lec3.2.8.1, a cell line deficient in N- and O-glycosylation (*20*). Stably transformed clonal cell lines were selected by their resistance to Geneticin and secretion of recombinant ZP3. Cells were seeded onto microbeads and grown in a 2.5 L, minicontinuous feeding−

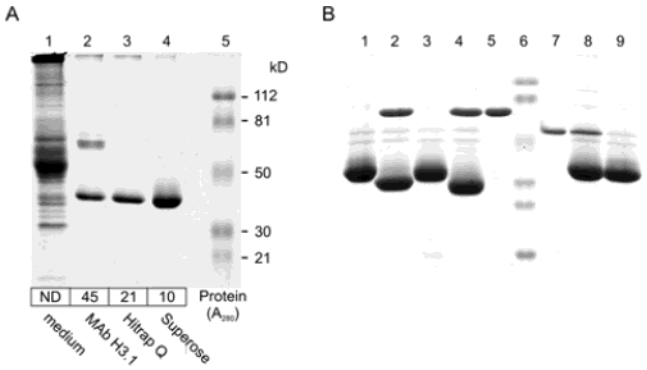

FIGURE 1: Characterization of purified recombinant human ZP3. (A) SDS−PAGE of recombinant human ZP3 recovered from each purification step. Lanes: 1, culture supernatant; 2, fractions eluted from H3.1 affinity column; 3, fractions collected from Hi-trap Q ion-exchange column; 4, fractions collected from Superose 12 gel filtration column after two separations; 5, molecular mass markers. Numbers below the gel reflect total protein recovery in the pooled human ZP3 fractions after the corresponding purification step measured as the total absorbance at 280 nm. (B) Purified recombinant human ZP3 (10 μg) was digested with glycosidase, separated by SDS−PAGE, and stained with Coomassie Brilliant Blue G. Lanes: 1, no treatment; 2, digestion with endo-H glycosidase; 3, digestion with O glycosidases; 4, digestion with endo-H and O glycosidases; 5, endo-H and O glycosidases alone; 6, molecular mass markers (112, 81, 50, 36, 30, 21 kDa); 7, furin alone; 8, human ZP3 digested with furin; 9, undigested human ZP3.

collecting culturing system enabling the collection of 200 L of supernatant during 3 months of culture. Aliquots of 20 L were concentrated, and recombinant human ZP3 was purified by affinity, ion-exchange, and gel filtration chromatography (Supporting Information, Figure 1).

SDS−PAGE and Coomassie Brilliant Blue G staining were used to track the purity of recombinant human ZP3 (~42 kDa) at each chromatographic step (Figure 1A). Affinity chromatography with the H3.1 monoclonal antibody removed most of the nontarget proteins either secreted by the cells or present in the culture medium (Figure 1A, lanes 1 and 2). The residual higher molecular weight bands (~60 kDa) were removed by Hi-trap Q ion-exchange chromatography (Figure 1A, lanes 2 and 3), and gel filtration removed aggregates of recombinant human ZP3 protein and the very high molecular weight contaminants at the top of the SDS−PAGE gel (Figure 1A, lanes 3 and 4). When the purified recombinant protein was reapplied to the Superose 12 gel filtration column, the profile (Supporting Information, Figure 1C) was consistent with a monodisperse solution of human ZP3. The total amount of protein recovered in the pooled human ZP3 fraction at each purification step was calculated by the absorbance at 280 nm (Figure 1A, bottom). From the initial 200 L of culture supernatant, 10 mg of ~95% pure recombinant human ZP3 was obtained.

Characterization of the Recombinant Human ZP3. The purified recombinant human ZP3 was further characterized by treatment with endoglycosidases (Figure 1B). Digestion with either endo-H glycosidase (Figure 1B, lane 2), endo-O glycosidase (in combination with neuraminidase) (Figure 1B, lane 3), or both (Figure 1B, lane 4) shifted the recombinant protein to a lower apparent molecular mass. The ability to digest recombinant human ZP3 with endo-H glycosidase indicates the presence of high mannose oligosaccharides and is consistent with reported glycosylation patterns of CHO-Lec3.2.8.1 cells (Figure 1A). Human ZP3 has four potential N-glycosylation sites, and the shift of ~4 kDa after treatment with PNGase F predicts that three of the four are occupied. The minimal shift in molecular mass after digestion with endo-O glycosidase and neuraminidase suggests that recombinant human ZP3 may have core 1 O-glycans (as predicted for expression in CHO-Lec3.2.8.1), but the extent of O-glycosylation is considerably less than N-glycosylation.

Human ZP3 has a potential proprotein convertase (furin) cleavage site (RXR/KR) upstream of the C-terminal transmembrane domain. The site is well conserved among zona pellucida proteins in other taxa and has been implicated in the release of ZP2 and ZP3 proteins during secretion (*28*, *29*). However, mutational inactivation of the furin site in mouse ZP3 or human ZP3 does not prevent secretion from heterologous cells nor incorporation into the extracellular zona pellucida in transgenic mice (*30*−*32*). Commercially obtained furin which cleaved anthrax protective antigen (*33*) in control experiments (data not shown) did not alter the apparent molecular mass after SDS−PAGE (Figure 1B, lanes 7−9). Taken together, these observations suggest that the C-terminus of the majority of secreted human ZP3 is either before or closely approximates the furin cleavage site.

Mass Spectrometric Analysis of Recombinant Human ZP3. Purified recombinant human ZP3 was reduced, alkylated, and deglycosylated with PNGase F alone or in combination with a mixture of de-exo and de-endo O-glycosidases. The former converts occupied asparagine to aspartic acid while leaving nonglycosylated asparagine residues intact, and the latter removes O-glycans. Samples were then digested with trypsin, Asp-N endoproteinase, or both prior to analysis by electrospray LC−MS. Additional nonreduced samples were analyzed to assist in the identification of disulfide bonds. Nearly complete coverage of recombinant human ZP3 was obtained (Supporting Information, Table 1).

N- and C-Termini. Both tryptic and Asp-N digestion of reduced and carbamidomethylated recombinant human ZP3 sample revealed $[M + 3H]^{3+}$ and $[M + 4H]^{4+}$ at *m*/*z* 1282.65 and 962.23 that match the N-terminal peptide ^{23}qPLWLLQGGASHPETSVQPVLVECQEATLMVMVSK^{57} with a pyroglutamate in place of a glutamine (Figure 2A). No CID was obtained in these cases. This N-terminal peptide was confirmed in a nonreduced sample in which the above peptide was disulfide-linked with ^{134}AEIPIECR^{141}, as evidenced by the 3+ and 4+ charges of this peptide at *m*/*z* 1572.78 and 1179.83 (Figure 2B). The CID spectrum of 1572.78^{3+} clearly showed the presence of y_{1-9} and b_{3-12} ions from P1 as well as y'_{1-4}, y'_6, and b'_{2-5} ions from P2 (Figure 2C; see ref *18* for nomenclature).

At the C-terminus, a similar cleavage to that in mouse ZP3 (i.e., two amino acid upstream of the furin cleavage site) occurred in human ZP3, giving rise to a carbamidomethylated peptide, ^{326}DCGTPSHSRRQPHVMSQWSRSASRN^{350}, as shown by the 4+ and 5+ charges of this peptide at *m*/*z* 731.84 and 585.67 from Asp-N endoproteinase cleavage (Figure 3A). Although the CID spectrum of 585.67^{5+} did not produce many fragment ions, most likely as a result of CID late in peak elution when less precursor ion signal was available, the presence of y_1, y_3, y_8-H_2O, and b_3 still confirmed the identity of the peptide (Figure 3B). However, there was evidence that the processing of full-length human ZP3 in heterologous CHO cells is more

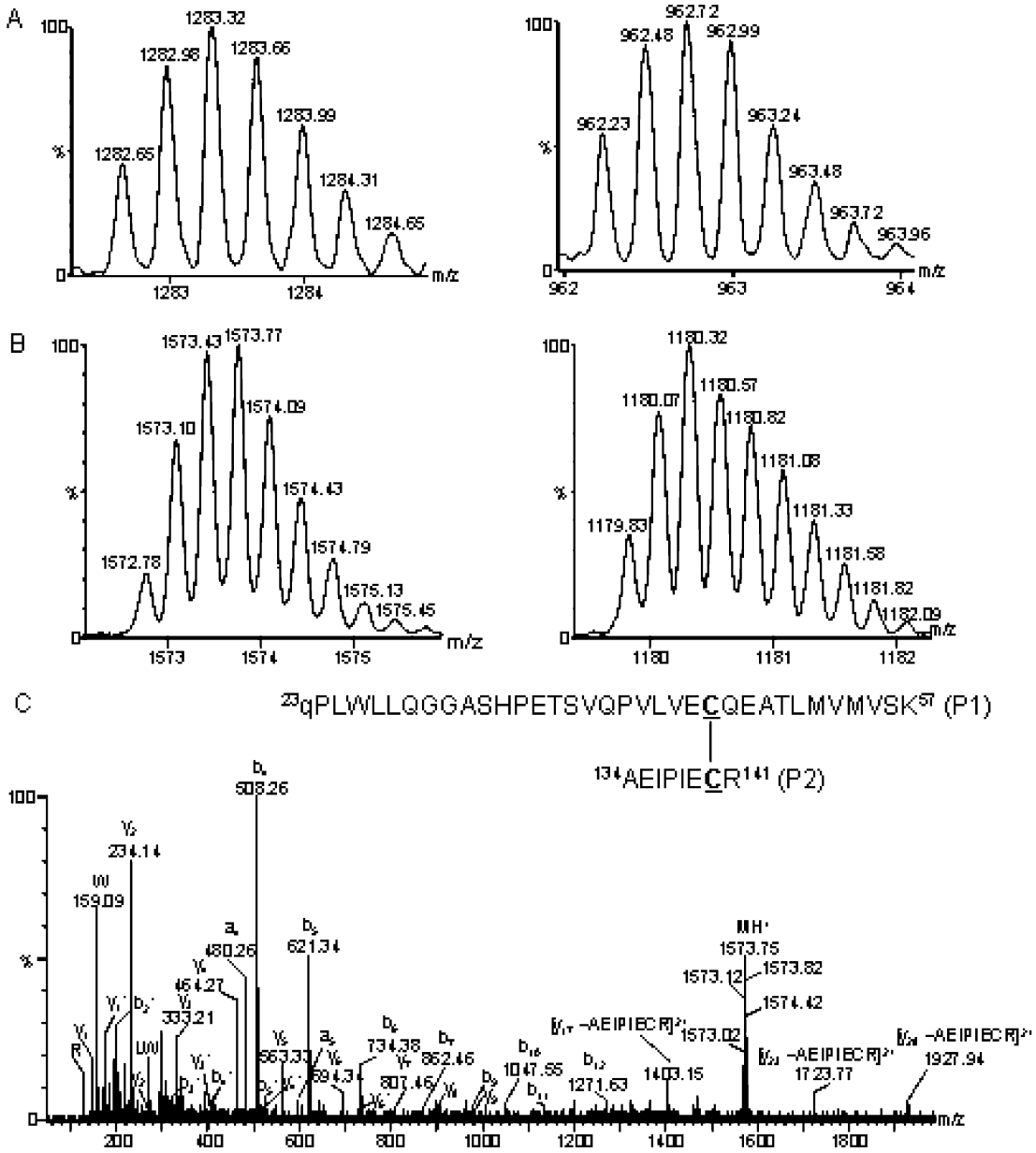

FIGURE 2: Determination of the N-terminus of recombinant human ZP3. (A) A carbamidomethylated N-terminal peptide ^{23}qPLWLLQGGASHPETSVQPVLVECQEATLMVMVSK^{57} with a pyroglutamate in place of glutamate. (B) The same N-terminal peptide disulfide-linked to ^{134}AEIPIECR^{141}. (C) CID spectrum of this disulfide-bonded peptide at m/z 1572.78^{3+}. Symbols y$^{\sim}$ and b$^{\sim}$ represent H_2O loss whereas y* and b* represent NH_3 loss. The ● symbol denotes disulfide linkage between y ions from P1 and the intact piece of P2. This nomenclature is also used in Figures 3−7 unless otherwise stated.

complicated than in the native mouse zona pellucida (*18*), since proteolytic peptides downstream of the furin site were observed with some even extending into the transmembrane domain. For example, a tryptic peptide, ^{353}HVTEEADVTVGPLIFLDR^{370} (m/z 671.02^{3+}; Figure 3C inset), was detected as well as an Asp-N endoproteinase cleaved peptide, ^{373}DHEVEQWALPS^{383} (m/z 655.81^{+2}; data not shown). The presence of these peptides suggests alternative C-terminal proteolytic processing during secretion of recombinant human ZP3 in CHO cells.

Disulfide Bonds. The mature human ZP3 protein contains 12 cysteine residues that are capable of forming six disulfide bonds, and all were experimentally determined to be disulfide-bridged (Table 1). In the first pair, masses corresponding to the N-terminal peptide ^{23}qPLWLLQGGASHPETSVQPVLVEC̲QEATLMVMVSK^{57} disulfide-linked to ^{134}AEIPIEC̲R^{141} were observed at m/z 1572.78^{3+} and 1179.83^{4+} from trypsin digestion as described above (Figure 2B,C). In the second pair (Figure 4B), a precursor ion of MH$^+$ 5921.77 as detected by its 5+ and 6+ charged ions at m/z 1185.13 and 987.79 corresponded to ^{68}AADLTLGPEAC̲EPLVSMDTEDVVR^{91} (P1) disulfide-bridged to ^{92}FEVGLHEC̲GNSMQVTDDALVYSTFLLHDPR^{121} (P2). The CID spectrum of m/z 987.79 yielded a y ion series including y_{1-12} ions carboxyl terminal to Cys^{78} of P1, as well as the b_{2-7} ions. In addition, P2 generated y'_{1-11} ions and sequential b ions including b'_{2-7} (Figure 4B).

Cys^{217}, Cys^{239}, Cys^{282}, and Cys^{300} form two disulfide bonds as shown by the ions at m/z 1253.19^{5+} and 1044.34^{6+} that represent a triply linked tryptic peptide with no information on the disulfide pattern (Table 1). Further digestion with Asp-N endoproteinase cleaved within this tryptic peptide

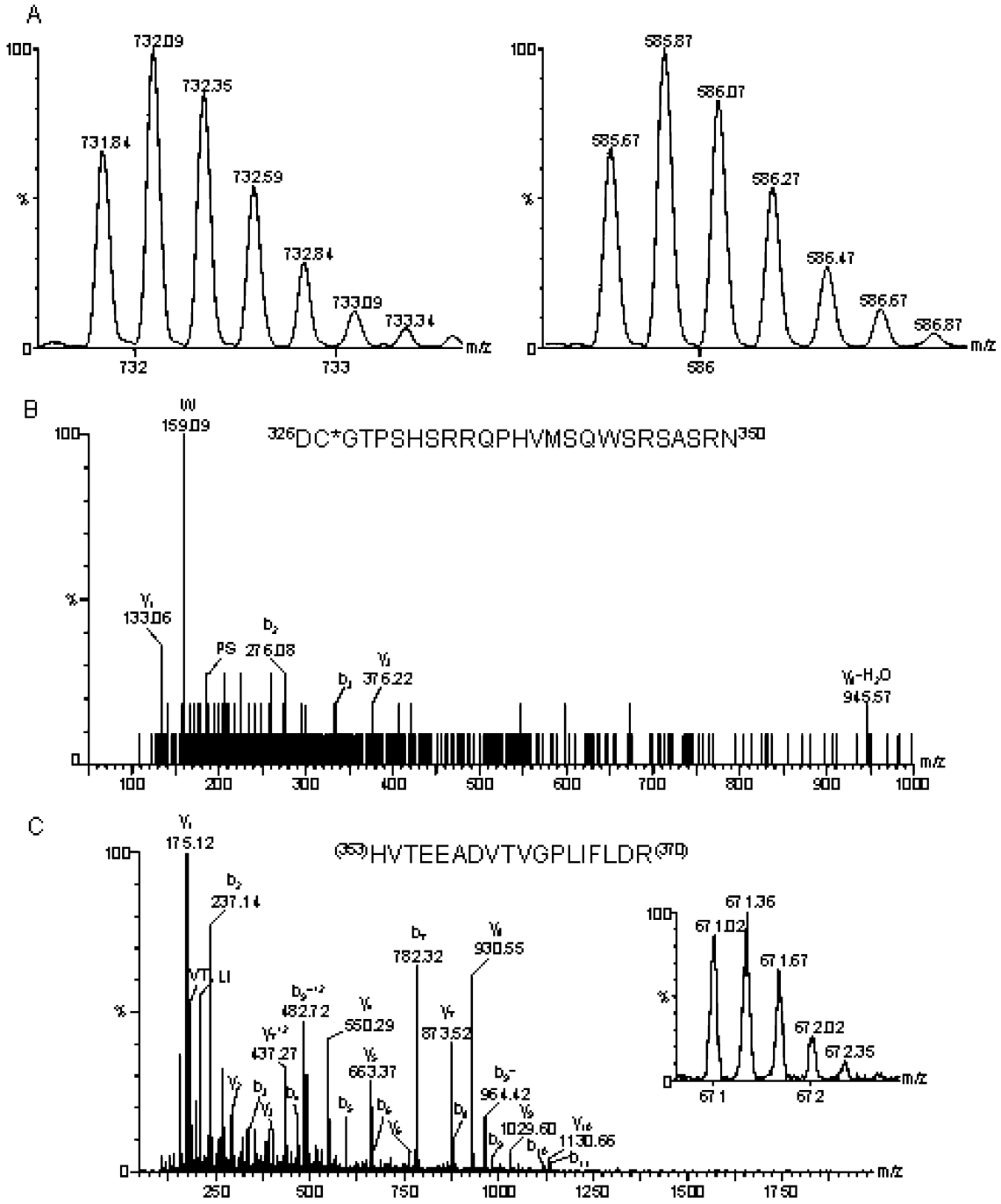

FIGURE 3: Determination of the C-terminus of recombinant human ZP3. (A) The 4+ and 5+ charges of a carbamidomethylated C-terminal peptide ^{326}DCGTPSHSRRQPHVMSQWSRSASRN^{350} from the Asp-N endoproteinase digest at *m*/*z* 731.84 and 585.67, similar to the C-terminus of native mouse ZP3 (i.e., two amino acids upstream of the furin site). (B) CID spectrum of *m*/*z* 731.84^{4+}. (C) CID spectrum of a trypsin-cleaved peptide ^{353}HVTEEADVTVGPLIFLDR^{370} (*m*/*z* 671.02^{3+}, inset) immediately downstream of the furin site was observed.

revealed the exact disulfide arrangement, i.e., Cys^{217}/Cys^{282} and Cys^{239}/Cys^{300}. The disulfide-linked peptides ^{215}DHC-VATPTP^{223} (P1) and ^{276}NMIYITCHLK^{285} (P2) were detected by the presence of ions at *m*/*z* 725.00^{3+} and 544.00^{4+}. In addition, the disulfide linkage between ^{235}DFHGCLV^{241} (P1) and ^{299}ACSFSK^{304} (P2) was confirmed by ions at *m*/*z* 477.20^{3+} and 358.15^{4+} (Table 1).

The four tightly clustered cysteines near the C-terminus form two more disulfide bonds between peptides ^{305}PSN-SWFPVEGPADICQCCNK^{324} and ^{325}GDCGTPSHAR^{334}, as indicated by the 3+ and 4+ charges of ions at *m*/*z* 1069.45 and 802.33 (MH$^+$ 3206.32) (Table 1). Since there was no enzyme cleavage site between the first three cysteines, the precise disulfide arrangement remains undetermined. The CID spectrum of 802.33^{4+} identified y_{1-2} and b_6 ions from P1, together with y'_{1-6} and [y_6−y_{14} disulfide-bonded to GDCGTPSHAR]$^{2+}$ (data not shown).

N-Glycosylation Sites. There are four potential N-linked glycosylation sites in mature human ZP3: Asn^{125}, Asn^{147}, Asn^{226}, and Asn^{272} (*3*). PNGase F endoglycosidase releases protein-bound N-linked glycans and by converting the involved asparagine residue to an aspartic acid provides a signature increase in mass (0.98 Da). Trypsin digestion generated three out of four Asn-containing peptides that have

Table 1: Disulfide Bond Linkage Mapping of Recombinant Human ZP3[a]

Residues	Sequences	Enzymes	m/z exp.	m/z calc.
23-57	qPLWLLQGGASHPETSVQPVLVECQEATLMVMVSK	Trypsin	1572.78^{3+} 1179.83^{4+}	1572.79^{3+} 1179.84^{4+}
134-141	AEIPIECR			
68-91	AADLTLGPEACEPLVSMDTEDVVR	Trypsin	987.79^{6+} 1185.13^{5+}	987.80^{6+} 1185.16^{5+}
92-121	FEVGLHECGNSMQVTDDALVYSTFLLHDPR			
212-252	LFVDHCVATPTPDQNASPYHTIVDFHGCLVDGLTDASSAFK	Trypsin	1044.34^{6+} 1253.19^{5+}	1044.33^{6+} 1253.20^{5+}
276-285	NMIYITCHLK			
299-304	ACSFSK			
235-241	DFHGCLV	Asp-N +Trypsin	358.15^{4+} 477.20^{3+}	358.16^{4+} 477.21^{3+}
299-304	ACSFSK			
215-223	DHCVATPTP	Asp-N +Trypsin	544.00^{4+} 725.00^{3+}	544.01^{4+} 725.01^{3+}
276-285	NMIYITCHLK			
305-324	PSNSWFPVEGPADICQCCNK	Trypsin	802.33^{4+} 1069.45^{3+}	802.34^{4+} 1069.44^{3+}
325-334	GDCGTPSHSR			

[a] q = pyroglutamate. Solid lines indicate the precise disulfide pairing, whereas dashed lines represent undetermined disulfide bonds.

been converted to aspartates after PNGase F deglycosylation (Table 2). A 2+ charged ion at *m*/*z* 478.28 represents the peptide ^{122}PVGNLSIVR^{130} where Asn^{125} has been converted to an aspartate (Figure 5A). The CID spectrum showed a complete sequence ion series (b_{2-8} and y_{1-8}) with b_{4-8} and y_{6-8} indicative of an Asn to Asp conversion (Figure 5B). Furthermore, a trace amount of a 2+ charged ion at *m*/*z* 477.80 was detected, suggesting that glycosylation at this site was incomplete. For Asn^{226}, however, no N-glycosylation was detected as shown by the 4+ and 5+ charges of the carbamidomethylated peptide ^{212}LFVDHCVATPTPDQNASPYHTIVDFHGCLVDGLTDASSAFK^{252} at *m*/*z* 1126.53 and 901.42. Confirming this, the nonreduced sample gave rise to a disulfide-bridged peptide between ^{212}LFVDHCVATPTPDQNASPYHTIVDFHGCLVDGLTDASSAFK^{252} and ^{276}NMIYITCHLK^{285}, which also contained an Asn instead of an Asp at position 226 (Table 2).

The last predicted N-glycosylation site lies at Asn^{272} (NDS). A tryptic peptide, ^{253}VPRPGPDTLQFTVDVFHFANDSR^{275}, shown as 3+ and 4+ charged ions at *m*/*z* 872.75 and 654.81, demonstrated a conversion from Asn to Asp as a result of PNGase F treatment. The CID spectrum of 872.75^{3+} not only confirmed the sequence by the presence of y_{1-11} ions but also located the original N-glycosylation site at Asn^{272}. Similarly, a population of nonglycosylated peptide was detected as 3+ and 4+ charged ions at *m*/*z* 872.45 and 654.57, again revealing the heterogeneity of the sample.

O-Glycosylation Sites. Despite nearly complete sequence coverage obtained from various digests, no information was available on residues 147−175 in the middle of the sequence, possibly due to O-glycosylation at a number of serine and threonine residues. Therefore, human ZP3 was treated with a combination of three exoglycosidases as previously described for native mouse zona pellucida proteins (*18*). After trypsinization, O-glycosylated peptides appeared bearing multiple core HexNAc·Hex residues (mass addition of 365.13 Da/HexNAc·Hex), as well as HexNAc·Hex plus *N*-acetylneuraminic (sialic) acid (291.3 Da/NANA). As shown in Table 3, a tryptic peptide, ^{145}QGNVSSQAILPTWLPFR^{161}, where Asn^{147} was converted to an Asp showed a 2+ charge at *m*/*z* 1140.55, 365.11 Da higher than its predicted mass (Figure 6A, inset). The CID spectrum on QTOF (Figure 6A) confirmed the sequence by y_1, y_{3-5}, y_{7-8}, y_{10}, b_{2-6}, and b_8, together with sugar marker ions described previously (*18*). Similarly, the site of O-glycan attachment was not determined due to the loss of the sugar moiety concurrent with peptide backbone cleavage. Therefore, lower collision energy (25% in an ion trap) was applied to this peptide to produce the fragmentation spectrum shown in Figure 6B. The most intense peaks are $[M\text{-Hex}]^{2+}$ and $[M\text{-(HexNAc·Hex)}]^{2+}$ at *m*/*z* 1059.8 and 958.3. In addition, a series of sequence ions including b_{4-10}, [b_{12}-(HexNAc·Hex)], [b_{13}-(HexNAc·Hex)], [b_{14}-(HexNAc·Hex)], [b_{16}-(HexNAc·Hex)], and y_{3-4} were produced. More importantly, y_{7-13} ions bearing Thr^{156} all showed a mass increase of 365.13 Da, confirming HexNAc·Hex attachment at this site and not at Ser^{148} or Ser^{149}.

The same low-energy CID experiment was performed on native mouse ZP3 where Thr^{155} was proposed as an O-glycosylation site (*18*). Figure 6C shows the tryptic peptide ^{144}QGNVSSHPIQPTWVPFR^{160} where Asn^{146} was converted to an Asp as a 3+ charged ion at *m*/*z* 772.70 (inset). The CID spectrum of this ion produced the most abundant ions as sugar losses from the peptide including $[M\text{-Hex}]^{3+}$ and $[M\text{-(HexNAc·Hex)}]^{2+}$ at *m*/*z* 719.2 and 976.4, along with its sugar signature ion of HexNAc·Hex + H^+ at *m*/*z* 366.0. The y_{7-8} ions at *m*/*z* 1267.6 and 1395.8 carrying an additional 365.13 Da indicate that Thr^{155} in mouse ZP3 is a site of O-glycosylation.

Additionally, there is a series of HexNAc·Hex additions (a maximum of three core sugars of 1095.39 Da) to the peptide ^{144}QGNVSSHPIQPTWVPFRTTVFSEEK^{169} or ^{144}QGNVSSHPIQPTWVPFRTTVFSEEKLTFSLR^{175} without definite assignment of up to three O-glycosylation sites out of six potential sites by CID (Table 3). This is most likely due to the large size of the peptides (one to two trypsin miscuts as a result of occupying O-glycans) and multiple labile glycosidic bonds. In fact, the most intense peaks in frag-

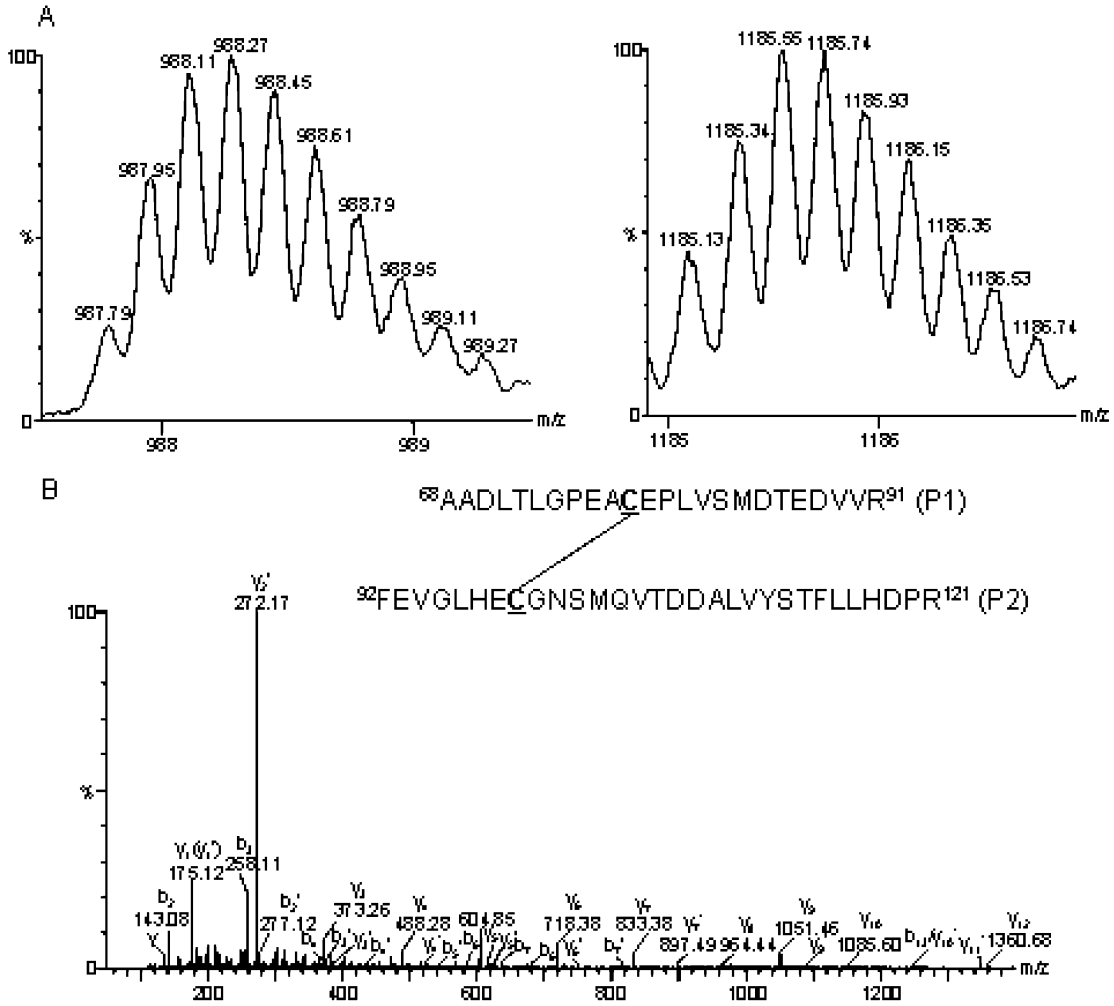

FIGURE 4: Disulfide bond linkage in recombinant human ZP3. Human ZP3 was digested with trypsin, the resultant peptides were detected by LC-QTOF, and CID was performed without DTT reduction. (A) A disulfide linkage between Cys^{78} and Cys^{99} is shown as the 5+ and 6+ charges at *m*/*z* 1185.13 and 987.79. (B) Sequence confirmation of this disulfide paired peptide by CID. The disulfide bonds of Cys^{46}/Cys^{140}, Cys^{78}/Cys^{99}, Cys^{217}/Cys^{282}, and Cys^{239}/Cys^{300} are indicated as solid lines in Table 1. Four cysteine residues (Cys^{319}, Cys^{321}, Cys^{322}, Cys^{327}) located too close together for a definitive determination of their linkages are indicated by dotted lines.

Table 2: LC−MS Analysis of Human ZP3 N-Linked Glycosylation Sites[a]

Residues	Sequences	Enzymes	m/z exp.	m/z calc.
122-130	PVG**N*LS**IVR	Trypsin	478.27^{2+}	477.79^{2+}
145-161	QG**N*VS**SQAILP**T**^WLPFR	Trypsin	1140.55^{2+}	1140.05^{2+}
212-252	LFVDHC*VATPTPDQNASPYHTIVDFHGCLVDGLTDASSAFK	Trypsin	1126.53^{4+} 901.42^{5+}	1126.53^{4+} 901.43^{5+}
212-252 276-285 299-304	LFVDHCVATPTPDQNASPYHTIVDFHGCLVDGLTDASSAFK NMIYITCHLK ACSFSK	Trypsin	1044.34^{6+} 1253.19^{5+}	1044.33^{6+} 1253.20^{5+}
253-275	VPRPGPDTLQFTVDVFHFA**N*DS**R	Trypsin	872.75^{3+} 654.81^{4+}	872.44^{3+} 654.58^{4+}

[a] **N*XS/T** represents N-linked asparagine converted to aspartate after PNGase treatment (+0.984 Da), whereas NXS/T is the predicted N-linked asparagine site but is experimentally determined to be nonglycosylated. ∧ = O-glycosylation sites. C* = carbamidomethylated cysteines. Note: All occupied N-glycosylation sites are partially glycosylated within the sample. All calculated masses for N-glycosylated peptides in tables are based on Asn and not Asp to indicate a mass shift of 0.98 Da after PNGase F digestion (experimental).

mentation were $[M\text{-}Hex]^{2+}$ and $[M\text{-}(HexNAc\cdot Hex)]^{2+}$ ions (spectra not shown). In one case, this same peptide carries not only three HexNAc·Hex moieties but also an *N*-acetylneuraminic acid (291.10 Da). Again, the precise O-glycosylation sites were not located by CID. Ser^{149} and Ser^{150} are less likely the sites due to the presence of b_{5-6} ions, although these ions could have lost their sugars during CID.

A second O-glycan cluster lies within a carbamidomethylated peptide, ^{256}PGPDTLQFTVDVFHFANDSRNMIYITCHLK^{285}, shown as a 4+ charged ion at *m*/*z* 1067.51 where Asn^{272} was not converted to an Asp (again reflecting

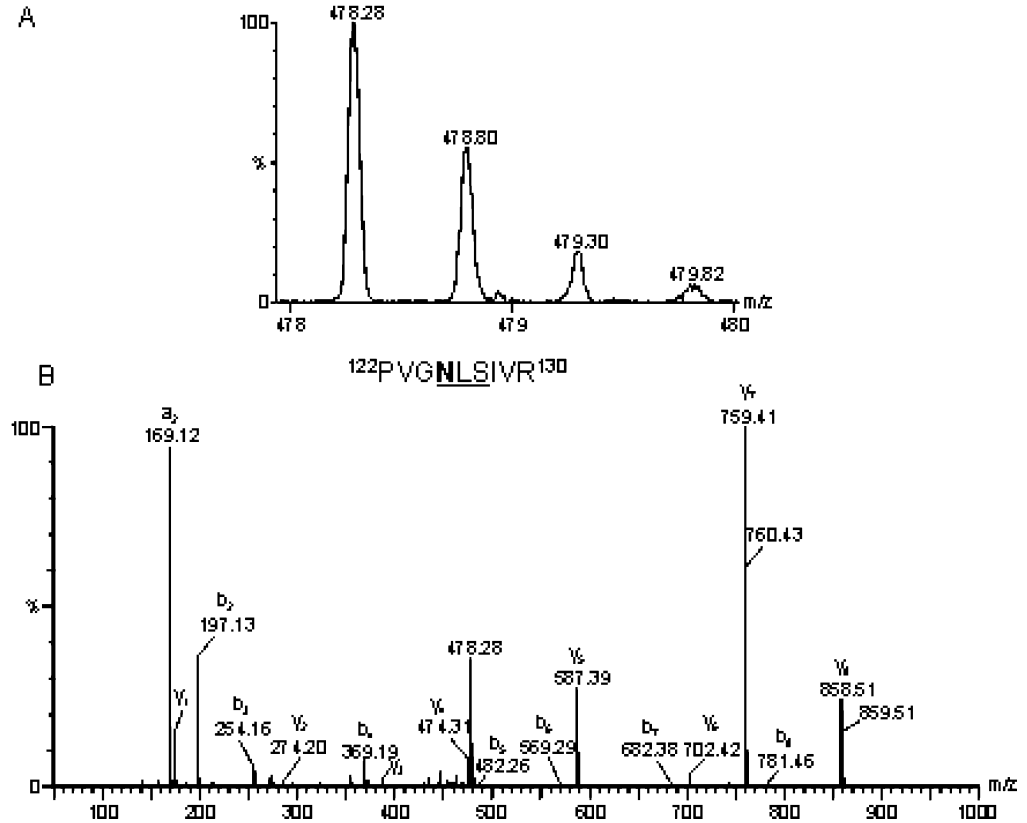

FIGURE 5: Localization of N-glycosylation sites in recombinant human ZP3. (A) The 2+ charge of an N-glycosylated peptide, ^{122}PVGNLSIVR^{130}, at *m*/*z* 478.28 where Asn^{125} was converted to Asp after PNGase treatment. (B) The CID spectrum of this peptide clearly indicated the replacement of Asn^{125} by Asp by y_{6-8} and b_{4-8} ions. The three N-linked glycosylation sites (Asn^{125}, Asn^{147}, Asn^{272}) are indicated in Table 2. The fourth potential N-linked glycosylation site (Asn^{226}) is not N-glycosylated.

Table 3: LC−MS Analysis of O-Glycosylation (Core O-Glycan Structures) on Human ZP3[a]

residues	sequences	*m*/*z* exptl	O-glycans	sites
145−161	QG**N*VS**SQAILP**T**∧WLPFR	1140.55^{2+}	1 HexNAc·Hex	T156
162−169	TTVFSEEK	653.28^{2+}	1 HexNAc·Hex	ND
145−169	QG**N*VS**SQAILPTWLPFRTTVFSEEK	1189.55^{3+}	2 HexNAc·Hex	ND
145−169	QG**N*VS**SQAILPTWLPFRTTVFSEEK	1311.25^{3+}	3 HexNAc·Hex	Ser149/Ser150[#]
		1966.35^{2+}		
145−169	QG**N*VS**SQAILPTWLPFRTTVFSEEK	1408.28^{3+}	3 HexNAc·Hex, 1 NANA	Ser149/Ser150[#]
145−175	QG**N*VS**SQAILPTWLPFRTTVFSEEKLTFSLR	1163.02^{4+}	3 HexNAc·Hex	Ser149/Ser150[#]
145−175	QG**N*VS**SQAILPTWLPFRTTVFSEEKLTFSLR	1235.84^{4+}	3 HexNAc·Hex, 1 NANA	Ser149/Ser150[#]
256−285	PGPDTLQFTVDVFHFANDSRNMIYITC*HLK	1067.51^{4+}	2 HexNAc·Hex	ND

[a] **S/T**∧ are O-glycosylation sites while the underline represents the region where O-glycosylation was detected. **N*XS/T** represents Asn residues converted to Asp after PNGase F removal of N-glycans. C* = carbamidomethylated cysteine. The underline denotes the region where multiple O-glycosylation sites most likely lie. ND = not determined. Ser149/Ser150[#] are less likely the O-glycan sites.

heterogeneity of the sample) and was 730.32 Da higher than predicted, indicating the presence of two HexNAc·Hex (Table 3). The sugar signature ions at *m*/*z* 204.09 and 366.15 and their corresponding H_2O losses dominate the CID spectrum of *m*/*z* 1067.51^{4+}, along with y_{1-2} and b_{2-3} ions without definitive indication of the precise O-glycan sites (data not shown). These findings were further corroborated by the chemical addition of methylamine to previously O-glycosylated Ser/Thr residues, which results in a 13 Da mass increment relative to nonglycosylated residues. However, the yield for this chemical reaction was either too low for CID selection or the converted peptides did not give satisfactory fragmentation, preventing assignment of specific O-glycan sites.

Sedimentation Equilibrium Analysis of Recombinant Human ZP3. The stoichiometry of the purified soluble protein was determined by sedimentation equilibrium. Data collected at a loading concentration of 0.14 A_{280} demonstrated that the sample is paucidisperse, and analysis in terms of a single ideal solute yielded an average buoyant molecular mass of 25300 ± 3000 Da (Table 4). The sample paucidispersity, as reflected by the large error in the molecular mass determination, may be a reflection of both heterogeneity in the N- and O-linked glycosylation and heterogeneity in C-terminal processing. Assuming that the human ZP3 is fully N- and O-glycosylated, namely, three N-linked Man_5 and on average three O-linked HexNAc·Hex chains, the sedimentation equilibrium data appear to be consistent with the presence of dimeric soluble human ZP3 (Table 4).

The sample paucidispersity may also be due to the presence of species other than a dimer in solution. Sedimentation equilibrium experiments at a loading concentration

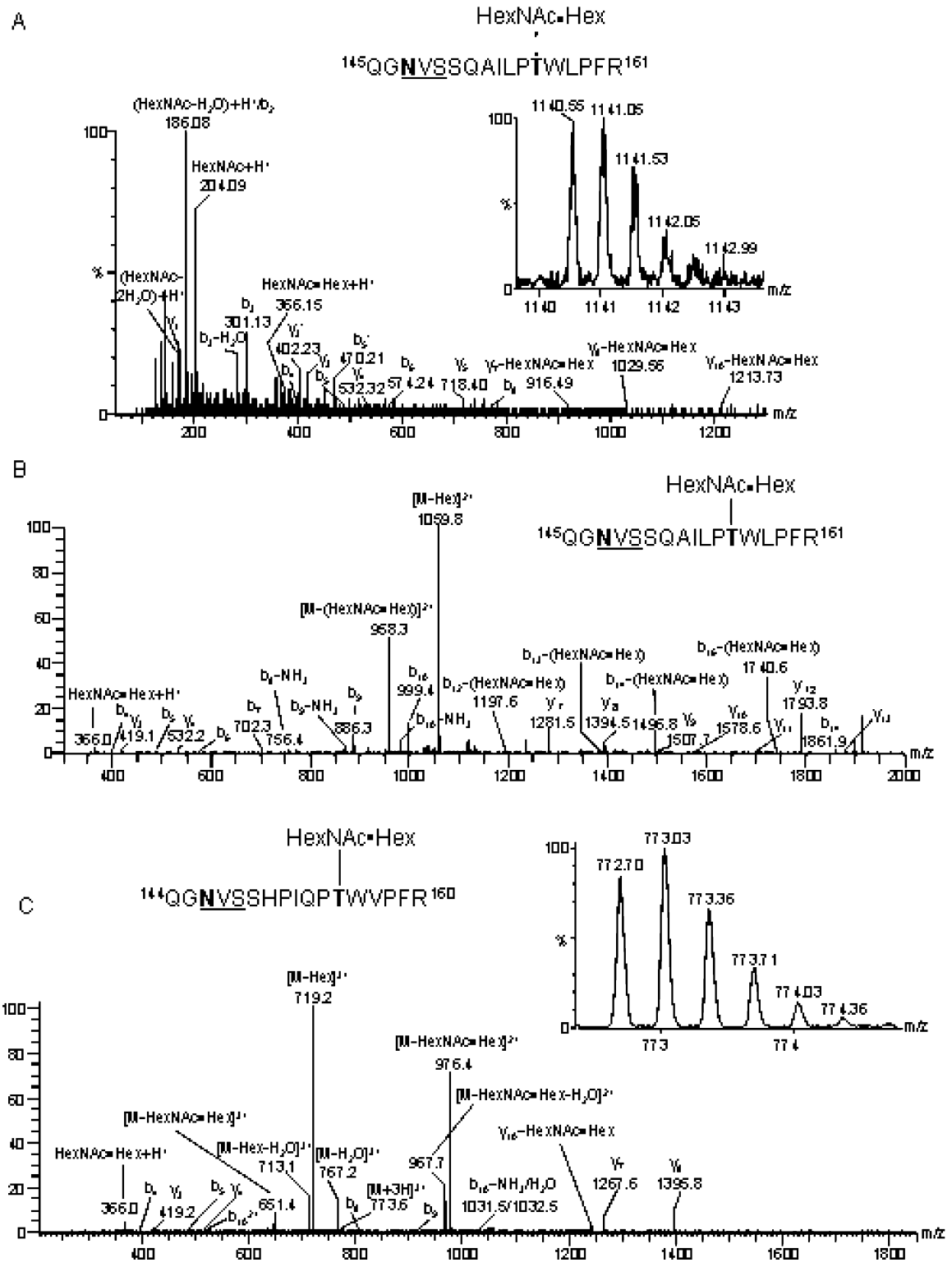

FIGURE 6: Identification of O-glycosylation in recombinant human ZP3. (A) An N- and O-glycosylated peptide, ^{145}QGN*VSSQAILPTWLPFR^{161}, that has a mass addition of 1 HexNAc·Hex (365.13 Da) at *m*/*z* 1140.55^{2+}. Its CID spectrum did not precisely assign the O-glycosylation site as sugars were readily lost during fragmentation as indicated by the dashed line. (B) Lower collision energy of the same peptide at *m*/*z* 1140.55^{2+} in an ion trap (25%) unequivocally located Thr^{156} as the site of sugar attachment due to the presence of y_{7-13} ions carrying 1 HexNAc·Hex. (C) The same lower energy CID experiment was performed on a similar peptide, ^{144}QGN*VSSHPIQPTWVPFR^{160}, in native mouse ZP3 at *m*/*z* 772.70^{3+} (inset). Again, Thr^{155} was determined to be the O-glycosylated site as shown by y_{7-8} ions bearing 1 HexNAc·Hex.

of 0.39 A_{280} confirmed this, and these data are best analyzed in terms of two single ideal solutes. An independent analysis of both the high and low concentration data sets in terms of two ideal solutes showed excellent data fits (Figure 7) and return a buoyant molecular mass of 21100 ± 210 Da for the predominant species. This result indicated that soluble human ZP3 is dimeric (Table 4) and was consistent with the observation that the C-terminal processing occurs primarily at Asn^{350}. The higher mass aggregate, which has a buoyant molecular mass of 55800 ± 3300 Da (n = 4.9 ± 0.3), is

Table 4: Characterization of Human ZP3 by Sedimentation Equilibrium

exptl $M(1 - \upsilon\rho)$/Da	residues	calcd $M_p(1 - \upsilon_p r)$/Da	calcd $M(1 - \upsilon\rho)$/Da	exptl stoichiometry
25300 ± 3000[a]	q23−N350	9673.2	11415[c]	2.22 ± 0.26
	q23−Q378	10575.3	12317[c]	2.05 ± 0.24
21100 ± 210[b]	q23−N350	9673.2	11415[c]	1.85 ± 0.02
	q23−N350	9673.2	10782[d]	1.96 ± 0.02

[a] Experimental buoyant molecular mass obtained by the simultaneous fitting of the low concentration data at different rotor speeds in terms of a single ideal solute. [b] Experimental buoyant molecular mass obtained by the simultaneous fitting of data at different rotor speeds in terms of two noninteracting ideal solutes. This is the buoyant molecular mass of the predominant species and is the value obtained from the analysis of both the low and high concentration experiments (Figure 8). [c] The calculated buoyant molecular mass is the sum of the protein and carbohydrate buoyant molecular masses. It is assumed that the ZP3 is N-glycosylated at three sites with Man_5 (H_5N_2, $M = 3 \times 1234.4$ Da, calculated $\upsilon_c = 0.63$ mL/g) and O-glycosylated at three sites with HexNAc·Hex ($M = 3 \times 365.1$ Da, calculated $\upsilon_c = 0.65$ mL/g). [d] It is assumed that the ZP3 is N-glycosylated at three sites with Man_3 (H_3N_2, $M = 3 \times 910.3$ Da, calculated $\upsilon_c = 0.64$ mL/g) and O-glycosylated at one site with HexNAc·Hex ($M = 365.1$ Da, calculated $\upsilon_c = 0.65$ mL/g).

present in concentrations of less than 5% that of the dimeric human ZP3 (Figure 7).

DISCUSSION

Mammals fertilize internally, and the evolutionary advantage of taxon-specific sperm binding is unclear. However, understanding the molecular details of this specificity may provide insight into the molecular basis of sperm−egg recognition. Initial biochemical analyses of human zonae pellucidae detected three glycoproteins (ZPB, ZP2, ZP3) with observed motilities on SDS−PAGE consistent with molecular masses of 64−78, 90−110, and 57−73 kDa, respectively (*27*, *34*). Mice also have three proteins (ZP1, ZP2, ZP3), but recent data suggest that human ZPB and mouse ZP1 are not homologues and that humans have a fourth zona protein more closely related to ZP1 (*35*). In mice, ZP3 is necessary (*13*, *14*), but not sufficient (*12*), for formation of the extracellular zona matrix in eggs, and although implicated as a sperm receptor (*36*, *37*), its role in sperm−egg recognition has become controversial (*17*, *38*). The current investigations were undertaken to compare human and mouse ZP3 to gain insight into its potential structural role in specifying taxon-specific sperm binding. Both human and mouse ZP3 are 424 amino acids in length with 67% identical residues. Both have identical signal peptide cleavage sites and share at least one carboxyl terminus. The conservation of 12 cysteine residues and the ordering of their disulfide bonds strongly suggest a common three-dimensional structure. The primary contribution to glycosylation is N-glycans, and the presence of three in human and five in mouse largely accounts for differences observed in the apparent molecular mass by SDS−PAGE of human (64 kDa) and mouse (83 kDa). Two patches of O-glycans are present in mouse ZP3, only one of which is detected in human, but O-glycans are consistently detected on human Thr^{156} and the corresponding mouse Thr^{155}. Neither human Ser^{331} nor Ser^{333}, homologues to mouse Ser^{332} and Ser^{334}, the glycosylation of which was previously implicated in sperm binding (*39*), is occupied by O-glycans (Figure 8). These data indicate that human and mouse ZP3 are quite similar and may not be the controlling determinants that account for the ability of human sperm to bind to human, but not mouse, zonae pellucidae.

To minimize heterogeneity for these analyses, recombinant human ZP3 was expressed in glycosylation-deficient CHO-Lec3.2.8.1 cells designed to limit N-linked glycosylation to five mannose residues attached to the core GlcNAc−GlcNAc disaccharide (±fucose) and O-linked glycosylation to a single *N*-acetylgalactosamine (*20*). Analyses of proteins expressed in these cells indicate that, in practice, N-glycans can range from Man_3 to Man_5 and that O-glycans (as noted with recombinant human ZP3) can contain core disaccharides (HexNAc·Hex), some with the addition of sialic acid. These observations appear to reflect incomplete penetrance of the Lec2 (defective CMP-sialic acid translocation) and Lec8 (defective UDP-galactose translocation) complementation phenotypes (*40*). Human ZP3 is present in the supernatant primarily as a dimer, and enzymatic removal of N-glycans results in microaggregation detected by sedimentation equilibrium ultracentrifugation (data not shown). Because of the paucity of recombinant protein recovered from the supernatant of cells grown in spinner flasks, the stably transformed cells were seeded onto microbeads that provide three-dimensional surface areas for attachment. Using a minicontinuous feeding−collecting system, ~10 mg of recombinant human ZP3 was purified by column chromatography, and microscale LC−MS was used to investigate the posttranslational modifications of secreted recombinant human ZP3.

The primary structure deduced from full-length cDNA predicts an N-terminal signal peptide (residues 1−22) and a transmembrane domain (residues 386-408) near the C-terminus (*3*). The current study confirms the cleavage of the signal peptide between residues 22−23 and demonstrates that the N-terminal glutamine of the secreted protein has been cyclized to pyroglutamic acid. Similar cylization of the N-terminal glutamine in mouse ZP1 and ZP3 is observed in native mouse zona pellucida (*18*). The zona pellucida is normally separated from the plasma membrane of the egg that it surrounds, and the ectodomain of human ZP3 needs to be released from the transmembrane domain (residues 387−408) to participate in the extracellular zona pellucida. A monoclonal antibody raised against a peptide epitope (residues 335−350) recognizes human ZP3 in the extracellular zona pellucida (*22*), indicating that cleavage must be C-terminal to this binding site. A potential proprotein endoprotease cleavage site (residues 349−352, RXR/KR↓) is ideally positioned upstream of the transmembrane domain and has been implicated in release of the ectodomain of mouse ZP3 (*28*, *29*). However, an EGFP-ZP3 fusion protein expressed in transgenic mice with an inactivating mutation of this site is incorporated into the zona pellucida (*32*), and, more pertinent to the current study, human ZP3 mutated in the furin site also is secreted, albeit less efficiently, from heterologous cells (*30*).

A previous mass spectrometric analysis of native mouse zona pellucida detected the C-termini of ZP1, ZP2, and ZP3, not at the preprotein convertase site (RXR/KR↓) but N-terminal to the dibasic motif (RX↓R/KR) within the site (*18*). Whether this is the actual cut site or whether cleavage at the furin site is followed by carboxylpeptidase activity, as has been suggested in quail, *Xenopus*, and pig homologues (*41*−*43*), remains to be determined. The further observation

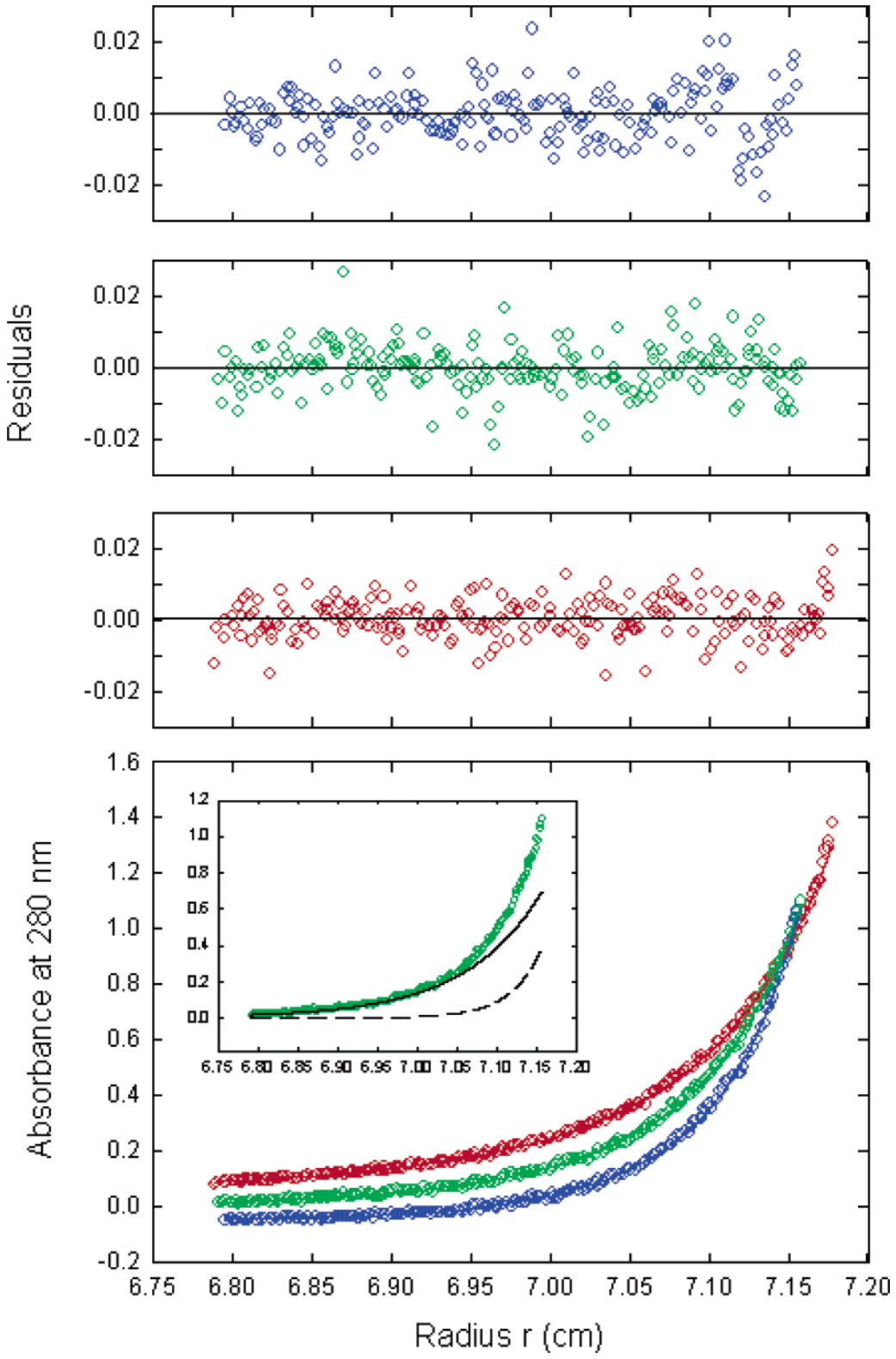

FIGURE 7: Stoichiometry of soluble human ZP3. Sedimentation equilibrium profiles at 280 nm and 4 °C for human ZP3 loaded at an A_{280} of 0.39 and collected at 10000 (red), 12000 (green) and 14000 (blue) rpm. The data collected at 10000 rpm have been shifted by +0.05 A_{280}, and those collected at 14000 rpm have been shifted by −0.05 A_{280} for clarity. The lines through the data represent the weighted best-fit global analysis in terms of two noninteracting ideal solutes. The distributions of the residuals to this fit are shown in the panels above. The inset shows the relative contributions of the human ZP3 dimer (solid line) and aggregate (dashed line) to the experimental data collected at 12000 rpm.

of secretion of mouse ZP3 mutated at the furin site (RNRR → ANAA) suggests other points of cleavage must be available as well (*32*). The detection of a recombinant human ZP3 peptide terminating at Asn^{350} (RN↓RR) after digestion with Asp-N endoproteinase is consistent with a C-terminus comparable to the Asn^{351} observed in native mouse ZP3 (Figure 8). Although the detection of at least two additional peptides C-terminal to this site indicates heterogeneity of

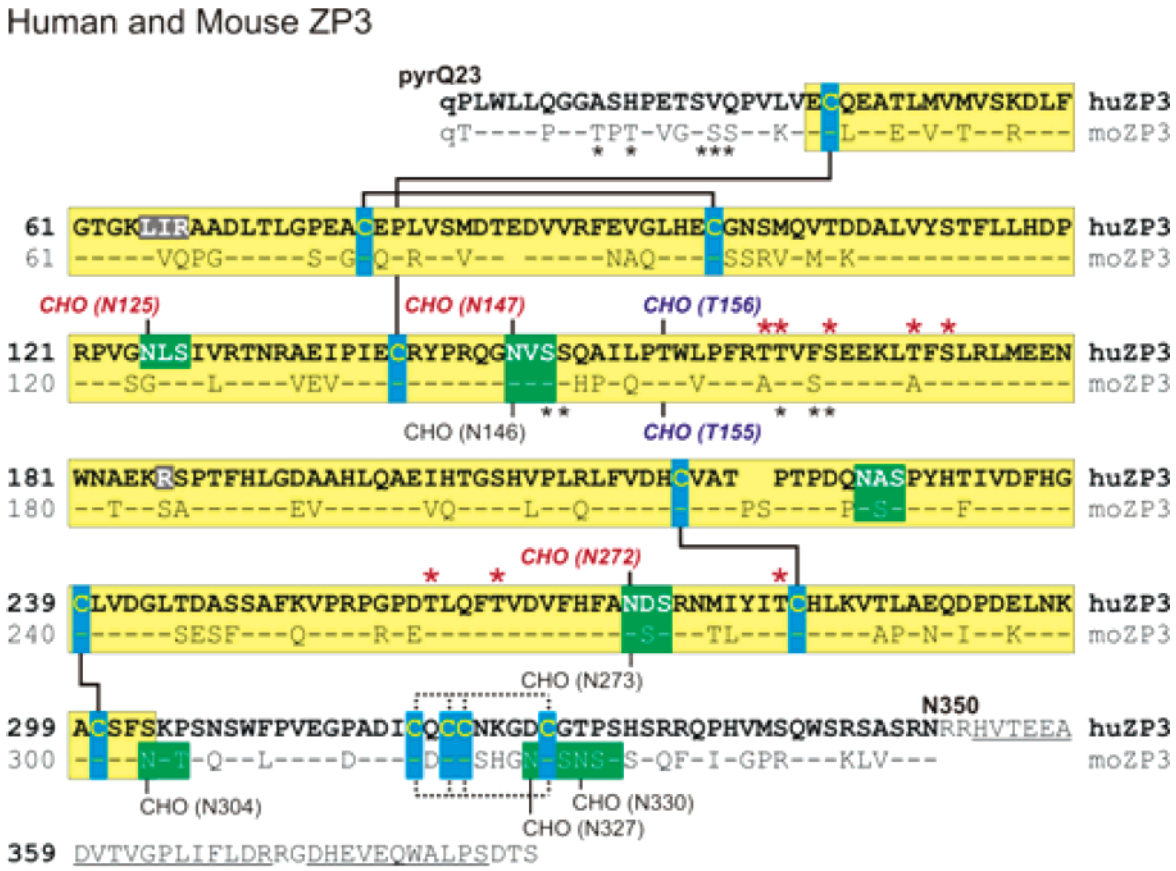

FIGURE 8: Comparison of native mouse and recombinant human ZP3. The primary amino acid sequence (single letter code) of recombinant human ZP3 is compared to native mouse ZP3. Amino acid residues that are identical are indicated by a dash in the mouse sequence. Four amino acids (white on gray background) in human ZP3 were not detected due to technical constraints. Both mouse and human ZP3 proteins begin with N-terminal pyroglutamates (pyrQ23), and although C-terminal heterogeneity of human ZP3 expressed in CHO-Lec3.2.8.1 is observed (e.g., H353−R370; D373−S383, underlined), an Asp-N peptide, ending in N350, corresponds to the C-terminus observed in native mouse ZP3 (N351). There are eight conserved cysteine (yellow on blue background) residues in the zona domain (yellow background) that are disulfide linked, C46/C140, C78/C99, C217/C282, and C239/C300 (solid line), as well as four cysteines (C319, C321, C322, C327) that are C-terminal to the zona domain. As in native mouse ZP3, the linkage of the latter (dotted lines) was indeterminate due to clustering of cysteine residues and the absence of appropriate cleavage sites. Three of the four potential N-linked sites in human ZP3 (white on green background) are glycosylated (shown in red; N125, N147, and N272 but not N226), and five previously determined N-glycans in mouse ZP3 are noted in black (N146, N273, N304, N327, and N330 but not N227). Two clusters of O-glycosylation were detected within residues 156−173 and 260−281 of human ZP3. In the first, an O-linked glycan is present at T156 (blue) with five additional potential sites (T162, T163, S166, T171, S173; red asterisks) nearby, and in the second, there are three sites (T260, T264, T281; red asterisks). Native mouse ZP3 was reanalyzed, and O-glycan occupancy was confirmed on T155 (blue); previously identified potential O-glycosylation sites on mouse ZP3 are indicated by black asterisks.

the cleavage site, the presence of a single human ZP3 band on SDS−PAGE (∼42 kDa) whose mobility does not change after digestion with furin (Figure 1B) suggests a single predominant C-terminus.

The mature human ZP3 protein has 12 cysteine residues that are capable of forming six disulfide bonds. By analyzing the mass spectra of enzymatic digests without reduction of cysteine residues, four disulfide bonds within the "zona domain" were unequivocally assigned, the arrangement of which is conserved between native mouse (*18*) and human (Figure 8). The first four human ZP3 cysteines (Cys^{46}/Cys^{140}, Cys^{78}/Cys^{99}) form a loop-within-loop motif (1−4, 2−3), and the second four (Cys^{217}/Cys^{282}, Cys^{239}/Cys^{300}) participate in a 1−3, 2−4 crossover motif. The remaining four cysteine residues (Cys^{319}, Cys^{321}, Cys^{322}, Cys^{327}) lie C-terminal to the zona domain and contain two disulfide bonds. Similar to native mouse ZP3 (*18*), they lie within a tight cluster (eight to nine amino acid residues), and the absence of proteolytic cleavage sites prevents precise assignment of disulfide bonds among the four with precision. The close proximity of four disulfide-bonded cysteine residues indicates a highly ordered secondary structure near the carboxyl terminus of the secreted protein that is conserved in mouse and human ZP3 but not the other zona proteins.

Zona pellucida proteins are glycosylated with both N- and O-linked carbohydrate side chains. The recognition sequence for N-linked glycosylation is Asn-Xaa-Ser/Thr, where Xaa is any amino acid except Pro. O-Linked glycosylation can potentially occur at any serine or threonine residue. The extent of glycosylation of human ZP3 was initially analyzed by mobility on SDS−PAGE before and after enzymatic removal of N- and O-linked oligosaccharide side chains. The recombinant protein secreted from CHO-Lec3.2.8.1 cells has an apparent molecular mass of ∼42 kDa. Treatment with N-glycosidase reduced the mass to ∼38 kDa, consistent with the presence of three Man_5 carbohydrate side chains attached to a GlcNAc disaccharide core (each ∼1.3 kDa). After digestion with O-glycosidases, there was minimal further decrease in molecular mass, suggesting that few of the serine and threonine residues were occupied by O-linked glycans.

These observations are in accord with the predicted mass of the native core polypeptide of ~36 kDa, and as observed with mouse ZP3 (*44*), human ZP3 appears more heavily N- than O-glycosylated.

Although glycoforms differing in N- and O-glycan occupancies (including nonglycosylated) are detected by mass spectrometry, the majority of the recombinant human ZP3 appears as a single band on SDS−PAGE run under nonreducing conditions prior to deglycosylation. Under reducing conditions, a second band is observed on SDS−PAGE that disappears after treatment with de-O glycosidases, confirming heterogeneity of O-glycan occupancy (data not shown). To determine sites of attachment, N-linked glycans were removed from human ZP3 with PNGase F, and the resultant deglycosylated peptides were identified by their predicted mass plus 0.98 mass unit for the expected alteration of the Asn to Asp. Alternatively, trypsinized ZP3 was treated with O-glycanases, and the detection of peptides not previously observed identified O-linked glycosylation sites. Human ZP3 contained four potential N-linked sites of which three were occupied (Asn^{125}, Asn^{147}, and Asn^{272}) similar to those (Asn^{124}, Asn^{146}, and Asn^{271}) detected biochemically in the pig homologue (*45*). Neither Asn^{226} in human ZP3 nor Asn^{225} in native mouse ZP3 (*18*) are glycosylated, perhaps because of adjacent proline residues. The net gain of two additional N-glycans in mouse ZP3 (Asn^{146}, Asn^{273}, Asn^{304}, Asn^{327}, Asn^{330}) results in the larger apparent molecular mass of the native zona protein (83 kDa) compared to human (64 kDa) and pig (55 kDa) ZP3 (*27*, *46*). Human ZP3 expressed in transgenic mouse oocytes has a molecular mass equivalent to native human ZP3 and distinct from mouse ZP3 (*22*), although O- and N-glycans attached by the mouse oocyte glycosylation machinery appear to be the same as endogenous mouse ZP3 (*47*). However, attachment sites were not reported, and whether the glycosylation patterns observed in recombinant human ZP3 (expressed in CHO-Lec3.2.8.1 or mouse oocytes) match those in native human ZP3 remains to be determined.

Of the 52 potential O-linked glycosylation sites in the mature human ZP3 protein, O-glycans were detected clustered in two regions: amino acid residues 156−173 and 260−281. In the first cluster, Thr^{156} was definitely glycosylated while five nearby residues (Thr^{162}, Thr^{163}, Ser^{166}, Thr^{171}, Ser^{173}) were heterogeneously occupied with zero to two additional O-glycans. Reexamination of the CID spectrum of native mouse ZP3 using lower energy confirmed O-glycan occupancy of the homologous Thr^{155} (*18*). The second cluster in recombinant human ZP3 contained three additional sites (Thr^{260}, Thr^{264}, Thr^{281}) that were heterogeneously occupied with one to two O-glycans. A fourth potential site (Ser^{274}) participates in the Asn^{272} recognition site (Asn-Asp-Ser) for an N-glycan and is presumably not available for occupancy (Figure 8).

To account for taxon-specific sperm binding, there must be either differences in individual zona components or differences in the organization of the components within the zona pellucida. The number of zona proteins differs among mammals, and the human matrix has a fourth protein, ZP4, that is not present in mouse (*5*, *35*). The other three proteins (ZP1, ZP2, ZP3) are well conserved, and the similarity between the structures of mouse and human ZP3 suggests that it does not account for taxon-specific sperm binding. Posttranslational glycosylation of individual zona proteins has been implicated in sperm binding, but the role of specific glycans remains controversial (*17*, *38*, *48*−*53*), and specific differences between mouse and human have not been determined. There also may be as yet-to-be-identified factor-(s) contributed during folliculogenesis that are important for postovulatory sperm binding. Thus, although the molecular basis of taxon-specific sperm−egg recognition in mammals remains indeterminate, continuing investigations into the difference between mouse and human zonae pellucidae may yet prove fruitful.

ACKNOWLEDGMENT

We thank the members of our laboratory for many useful discussions and appreciate the critical reading of the manuscript by Dr. Douglas Sheeley.

SUPPORTING INFORMATION AVAILABLE

One table providing LC−MS and MS/MS analysis of human ZP3 and one figure showing the purification of recombinant human ZP3 by glycosylation-deficient CHO-Lec cells. This material is available free of charge via the Internet at http://pubs.acs.org.

REFERENCES

1. Yanagimachi, R. (1994) in *The Physiology of Reproduction* (Knobil, E., and Neil, J., Eds.) pp 189−317, Raven Press, New York.
2. Liang, L.-F., and Dean, J. (1993) Conservation of the mammalian secondary sperm receptor genes results in promoter function of the human homologue in heterologous mouse oocytes, *Dev. Biol. 156*, 399−408.
3. Chamberlin, M. E., and Dean, J. (1990) Human homolog of the mouse sperm receptor, *Proc. Natl. Acad. Sci. U.S.A. 87*, 6014−6018.
4. Harris, J. D., Hibler, D. W., Fontenot, G. K., Hsu, K. T., Yurewicz, E. C., and Sacco, A. G. (1994) Cloning and characterization of zona pellucida genes and cDNAs from a variety of mammalian species: ZPA, ZPB, and ZPC gene families, *DNA Sequence 4*, 361−393.
5. Hughes, D. C., and Barratt, C. L. (1999) Identification of the true human orthologue of the mouse Zp1 gene: evidence for greater complexity in the mammalian zona pellucida?, *Biochim. Biophys. Acta 1447*, 303−306.
6. Rankin, T., and Dean, J. (2000) The zona pellucida: Using molecular genetics to study the mammalian egg coat, *Rev. Reprod. 5*, 114−121.
7. Bork, P., and Sander, C. (1992) A large domain common to sperm receptors (Zp2 and Zp3) and TGF-beta type III receptor, *FEBS Lett. 300*, 237−240.
8. Killick, R., Legan, P. K., Malenczak, C., and Richardson, G. P. (1995) Molecular cloning of chick beta-tectorin, an extracellular matrix molecule of the inner ear, *J. Cell Biol. 129*, 535−547.
9. Legan, P. K., Rau, A., Keen, J. N., and Richardson, G. P. (1997) The mouse tectorins. Modular matrix proteins of the inner ear homologous to components of the sperm-egg adhesion system, *J. Biol. Chem. 272*, 8791−8801.
10. Jovine, L., Qi, H., Williams, Z., Litscher, E., and Wassarman, P. M. (2002) The ZP domain is a conserved module for polymerization of extracellular proteins, *Nat. Cell Biol. 4*, 457−461.
11. Rankin, T., Talbot, P., Lee, E., and Dean, J. (1999) Abnormal zonae pellucidae in mice lacking ZP1 result in early embryonic loss, *Development 126*, 3847−3855.
12. Rankin, T. L., O'Brien, M., Lee, E., Wigglesworth, K. E. J. J., and Dean, J. (2001) Defective zonae pellucidae in *Zp2* null mice disrupt folliculogenesis, fertility and development, *Development 128*, 1119−1126.
13. Liu, C., Litscher, E. S., Mortillo, S., Sakai, Y., Kinloch, R. A., Stewart, C. L., and Wassarman, P. M. (1996) Targeted disruption of the *mZP3* gene results in production of eggs lacking a zona

pellucida and infertility in female mice, *Proc. Natl. Acad. Sci. U.S.A. 93*, 5431−5436.
14. Rankin, T., Familari, M., Lee, E., Ginsberg, A. M., Dwyer, N., Blanchette-Mackie, J., Drago, J., Westphal, H., and Dean, J. (1996) Mice homozygous for an insertional mutation in the *Zp3* gene lack a zona pellucida and are infertile, *Development 122*, 2903−2910.
15. McLeskey, S. B., Dowds, C., Carballada, R., White, R. R., and Saling, P. M. (1998) Molecules involved in mammalian sperm-egg interaction, *Int. Rev. Cytol. 177*, 57−113.
16. Wassarman, P. M., Jovine, L., and Litscher, E. S. (2001) A profile of fertilization in mammals, *Nat. Cell Biol. 3*, E59−E64.
17. Dean, J. (2004) Reassessing the molecular biology of sperm-egg recognition with mouse genetics, *BioEssays 26*, 29−38.
18. Boja, E. S., Hoodbhoy, T., Fales, H. M., and Dean, J. (2003) Structural characterization of native mouse zona pellucida proteins using mass spectrometry, *J. Biol. Chem. 278*, 34189−34202.
19. Beebe, S. J., Leyton, L., Burks, D., Fuerst, T., Dean, J., and Saling, P. M. (1992) Recombinant ZP3 inhibits sperm binding and induces the acrosome reaction, *Dev. Biol. 151*, 48−54.
20. Stanley, P. (1989) Chinese hamster ovary cell mutants with multiple glycosylation defects for production of glycoproteins with minimal carbohydrate heterogeneity, *Mol. Cell. Biol. 9*, 377−383.
21. Kaufman, J. B., Wang, G., Zhang, W., Valle, M. A., and Shiloach, J. (2000) Continuous production and recovery of recombinant Ca^{2+} binding receptor from HEK 293 cells using perfusion through packed bed bioreactor, *Cytotechnology 33*, 3−11.
22. Rankin, T. L., Tong, Z.-B., Castle, P. E., Lee, E., Gore-Langton, R., Nelson, L. M., and Dean, J. (1998) Human *ZP3* restores fertility in *Zp3* null mice without affecting order-specific sperm binding, *Development 125*, 2415−2424.
23. Hanisch, F. G., Jovanovic, M., and Peter-Katalinic, J. (2001) Glycoprotein identification and localization of O-glycosylation sites by mass spectrometric analysis of deglycosylated/alkylaminylated peptide fragments, *Anal. Biochem. 290*, 47−59.
24. Ghirlando, R., Keown, M. B., Mackay, G. A., Lewis, M. S., Unkeless, J. C., and Gould, H. J. (1995) Stoichiometry and thermodynamics of the interaction between the Fc fragment of human IgG1 and its low-affinity receptor Fc gamma RIII, *Biochemistry 34*, 13320−13327.
25. Perkins, S. J. (1986) Protein volumes and hydration effects. The calculations of partial specific volumes, neutron scattering match-points and 280-nm absorption coefficients for proteins and glycoproteins from amino acid sequences, *Eur. J. Biochem. 157*, 169−180.
26. Durchschlag, H. (1986) in *Thermodynamic Data for Biochemistry and Biotechnology* (Hinz, H.-J., Ed.) pp 45−128, Springer-Verlag, Berlin.
27. Shabanowitz, R. B., and O'Rand, M. G. (1988) Characterization of the human zona pellucida from fertilized and unfertilized eggs, *J. Reprod. Fertil. 82*, 151−161.
28. Yurewicz, E. C., Hibler, D., Fontenot, G. K., Sacco, A. G., and Harris, J. (1993) Nucleotide sequence of cDNA encoding ZP3 alpha, a sperm-binding glycoprotein from zona pellucida of pig oocyte, *Biochim. Biophys. Acta 1174*, 211−214.
29. Williams, Z., and Wassarman, P. M. (2001) Secretion of mouse ZP3, the sperm receptor, requires cleavage of its polypeptide at a consensus furin cleavage-site, *Biochemistry 40*, 929−937.
30. Kiefer, S. M., and Saling, P. (2002) Proteolytic processing of human zona pellucida proteins, *Biol. Reprod. 66*, 407−414.
31. Qi, H., Williams, Z., and Wassarman, P. M. (2002) Secretion and assembly of zona pellucida glycoproteins by growing mouse oocytes microinjected with epitope-tagged cDNAs for mZP2 and mZP3, *Mol. Biol. Cell 13*, 530−541.
32. Zhao, M., Gold, L., Ginsberg, A. M., Liang, L.-F., and Dean, J. (2002) Conserved furin cleavage site not essential for secretion and integration of ZP3 into the extracellular egg coat of transgenic mice, *Mol. Cell. Biol. 22*, 3111−3120.
33. Gordon, V. M., Klimpel, K. R., Arora, N., Henderson, M. A., and Leppla, S. H. (1995) Proteolytic activation of bacterial toxins by eukaryotic cells is performed by furin and by additional cellular proteases, *Infect. Immun. 63*, 82−87.
34. Bauskin, A. R., Franken, D. R., Eberspaecher, U., and Donner, P. (1999) Characterization of human zona pellucida glycoproteins, *Mol. Reprod. Dev. 5*, 534−540.
35. Lefièvre, L., Conner, S. J., Salpekar, A., Olufowobi, O., Ashton, P., Pavlovic, B., Lenton, W., Afnan, M., Brewis, I. A., Monk, M., Hughes, D. C., and Barratt, C. L. R. (2004) Four zona pellucida glycoprotesin are expressed in the human, *Hum. Reprod. 19*, 1580−1586.
36. Bleil, J. D., and Wassarman, P. M. (1980) Mammalian sperm-egg interaction: Identification of a glycoprotein in mouse egg zonae pellucidae possessing receptor activity for sperm, *Cell 20*, 873−882.
37. Wassarman, P. M. (2002) Sperm receptors and fertilization in mammals, *Mt. Sinai J. Med. 69*, 148−155.
38. Rankin, T. L., Coleman, J. S., Epifano, O., Hoodbhoy, T., Turner, S. G., Castle, P. E., Lee, E., Gore-Langton, R., and Dean, J. (2003) Fertility and taxon-specific sperm binding persist after replacement of mouse 'sperm receptors' with human homologues, *Dev. Cell 5*, 33−43.
39. Chen, J., Litscher, E. S., and Wassarman, P. M. (1998) Inactivation of the mouse sperm receptor, mZP3, by site-directed mutagenesis of individual serine residues located at the combining site for sperm, *Proc. Natl. Acad. Sci. U.S.A. 95*, 6193−6197.
40. Merry, A. H., Gilbert, R. J., Shore, D. A., Royle, L., Miroshnychenko, O., Vuong, M., Wormald, M. R., Harvey, D. J., Dwek, R. A., Classon, B. J., Rudd, P. M., and Davis, S. J. (2003) O-glycan sialylation and the structure of the stalk-like region of the T cell co-receptor CD8, *J. Biol. Chem. 278*, 27119−27128.
41. Sasanami, T., Pan, J., Doi, Y., Hisada, M., Kohsaka, T., and Toriyama, M. (2002) Secretion of egg envelope protein ZPC after C-terminal proteolytic processing in quail granulosa cells, *Eur. J. Biochem. 269*, 2223−2231.
42. Kubo, H., Matsushita, M., Kotani, M., Kawasaki, H., Saido, T. C., Kawashima, S., Katagiri, C., and Suzuki, A. (1999) Molecular basis for oviductin-mediated processing from gp43 to gp41, the predominant glycoproteins of Xenopus egg envelopes, *Dev. Genet. 25*, 123−129.
43. Yonezawa, N., and Nakano, M. (2003) Identification of the carboxyl termini of porcine zona pellucida glycoproteins ZPB and ZPC, *Biochem. Biophys. Res. Commun. 307*, 877−882.
44. Nagdas, S. K., Araki, Y., Chayko, C. A., Orgebin-Crist, M.-C., and Tulsiani, D. R. P. (1994) O-linked trisaccharide and N-Linked poly-*N*-acetyllactosaminyl glycans are present on mouse ZP2 and ZP3, *Biol. Reprod. 51*, 262−272.
45. Yonezawa, N., Fukui, N., Kudo, K., and Nakano, M. (1999) Localization of neutral N-linked carbohydrate chains in pig zona pellucida glycoprotein ZPC, *Eur. J. Biochem. 260*, 57−63.
46. Yurewicz, E. C., Sacco, A. G., and Subramanian, M. G. (1987) Structural characterization of the Mr = 55, 000 antigen (ZP3) of porcine oocyte zona pellucida. Purification and characterization of alpha- and beta-glycoproteins following digestion of lactosaminoglycan with endo-beta-galactosidase, *J. Biol. Chem. 262*, 564−571.
47. Dell, A., Chalabi, S., Easton, R. L., Haslam, S. M., Sutton-Smith, M., Patankar, M. S., Lattanzio, F., Panico, M., Morris, H. R., and Clark, G. F. (2003) Murine and human zona pellucida 3 derived from mouse eggs express identical O-glycans, *Proc Natl. Acad. Sci. U.S.A. 100*, 15631−15636.
48. Thall, A. D., Maly, P., and Lowe, J. B. (1995) Oocyte gal alpha 1,3gal epitopes implicated in sperm adhesion to the zona pellucida glycoprotein ZP3 are not required for fertilization in the mouse, *J. Biol. Chem. 270*, 21437−21440.
49. Liu, D. Y., Baker, H. W., Pearse, M. J., and d'Apice, A. J. (1997) Normal sperm-zona pellucida interaction and fertilization in vitro in alpha-1,3-galactosyltransferase gene knockout mice, *Mol. Hum. Reprod. 3*, 1015−1016.
50. Asano, M., Furukawa, K., Kido, M., Matsumoto, S., Umesaki, Y., Kochibe, N., and Iwakura, Y. (1997) Growth retardation and early death of beta-1,4-galactosyltransferase knockout mice with augmented proliferation and abnormal differentiation of epithelial cells, *EMBO J. 16*, 1850−1857.
51. Lu, Q., and Shur, B. D. (1997) Sperm from β1,4-galactosyltransferase-null mice are refractory to ZP3-induced acrosome reactions and penetrate the zona pellucida poorly, *Development 124*, 4121−4131.
52. Ellies, L. G., Tsuboi, S., Petryniak, B., Lowe, J. B., Fukuda, M., and Marth, J. D. (1998) Core 2 oligosaccharide biosynthesis distinguishes between selectin ligands essential for leukocyte homing and inflammation, *Immunity 9*, 881−890.
53. O'Donnell, N., Zachara, N. E., Hart, G. W., and Marth, J. D. (2004) Ogt-dependent X-chromosome-linked protein glycosylation is a requisite modification in somatic cell function and embryo viability, *Mol. Cell. Biol. 24*, 1680−1690.

BI048958K